

15 **Abstract**

16 Recent world-wide quieting of seismic noise caused by COVID-19 lockdown measures has been
17 observed by seismometers. However, current seismic network that has a few seismometers or
18 none in a city-scale area is hard to reveal the spatiotemporal characteristic of seismic noise
19 impacted by COVID-19 measures. Here, we show that a 5-km-long distributed acoustic sensing
20 (DAS) array deployed in State College, PA is able to illuminate seismic noise variation in a
21 broad bandwidth 0.01 – 100 Hz during March – June 2020. The temporal noise variation exhibits
22 a ‘decrease-increase’ trend responding to ‘decrease-increase’ human activities caused by the
23 COVID-19 measures – from stay-at-home to Phase Green. Our results reveal different types of
24 human activities (including footsteps, road traffics, and machines) as noise sources, suggesting
25 that DAS noise recordings using cite widely-installed infrastructure fiber optics could be used for
26 quantifying the impact of COVID-19 measures on human activities in city block dimensions.
27

28 **Plain Language Summary**

29 COVID-19 lockdown measures make the world quieter since people stay at home and make
30 fewer noises. Current seismic networks can only detect the noise level averagely in urban areas.
31 Distributed Acoustic Sensing (DAS) can convert existing telecommunication optic fibers that
32 have been widely installed in the city in past decades into dense seismic sensors and provide high
33 spatiotemporal resolution monitoring of seismic noise. Here we show the noise level changes
34 caused by progressive COVID-19 measures from a 5-km-long fiber array deployed in the city of
35 State College, PA. We find the same decrease-increase trend in both noise level and human
36 activities. We distinguish noise generated by different types of human activities including
37 footsteps, road traffics, and machines. This study shows that DAS can be used to track human
38 activity with highly spatial resolution.

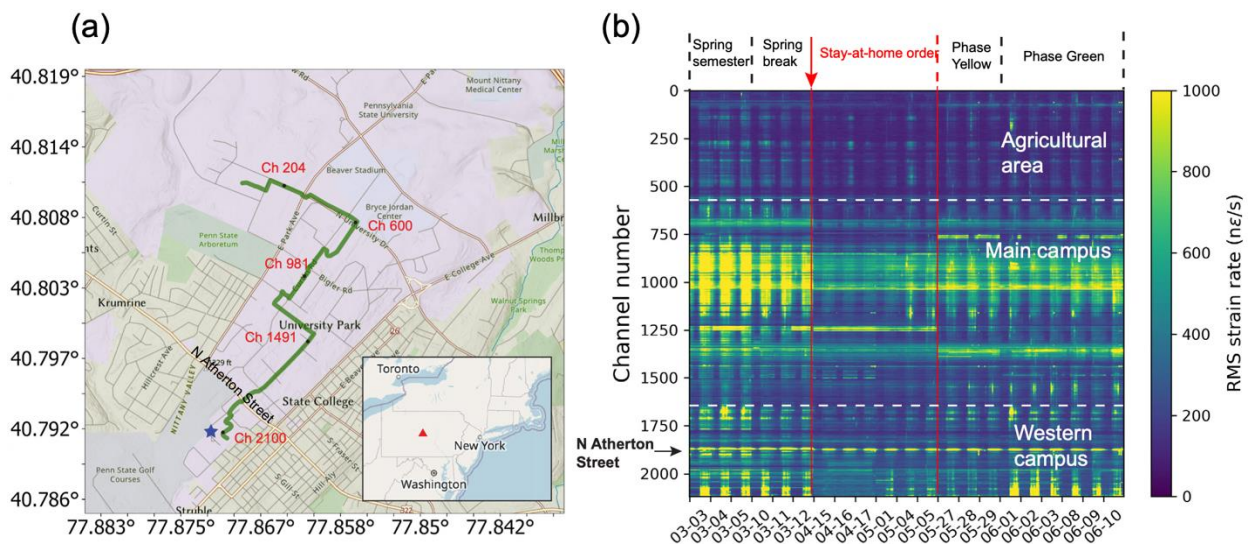
39 **1 Introduction**

40 COVID-19 pandemic has been impacting all aspects of our society particularly on public health
41 and economy. To reduce the spread of coronavirus, the COVID-19 measures such as working
42 from home, self-isolation, and community contact reduction were implemented and resulted in
43 the severe disruption in human activities. In the initial stage of the pandemic, the lockdown
44 measures were adopted regionally and globally, resulting in less human activities; After adopting
45 the loose measure re-opening schools and the economy gradually increases human activities.
46 Therefore, quantifying human activities may serve a potential way to evaluate the effectiveness
47 of the measures and optimize measures in the future (Gupta et al., 2020; Jarvis et al., 2020).

48 Seismologically, human activities generate vibration noises with frequency above 1 Hz (referred
49 to anthropogenic noise) (Bonney-Claudet et al., 2006; Xiao et al., 2020). Several recent reports
50 have shown that after COVID-19 lockdown seismometers detected a significant drop of high-
51 frequency anthropogenic noise levels (roughly 1-20 Hz) directly corresponding to less human
52 activities in the urban cities in the wide world (Xiao et al., 2020; Poli et al., 2020; Lecocq et al.,
53 2020; Dias et al., 2020; Yabe et al., 2020). These studies commonly use seismic stations
54 designed for recording low frequency earthquakes to track lockdown induced seismic noise
55 changes. Apparently, a few seismometers (or even none) in many cities pose a technical
56 challenge to characterize high-frequency seismic noise with a desired spatial and temporal
57 resolution, considering highly spatial-varying and temporal-varying noises in urban
58 environments.

59 Distributed acoustic sensing (DAS), a recent technology converting optic fibers to dense seismic
 60 sensor arrays, could provide high fidelity seismic strain/strain rate measurements at the meter
 61 spacing (Lindsey et al., 2017; Ajo-Franklin et al., 2019; Zhan et al., 2020). By using existing
 62 telecommunications infrastructure, particularly by plugging into "dark" or unused fiber that is
 63 already installed underground, these experiments greatly reduce the experimental cost and setup
 64 time as an interrogator simply needs to be plugged into one end of a stretch of fiber to being data
 65 acquisition. DAS has been demonstrated with tens of kilometers long telecommunication fiber
 66 cables for seismic monitoring (Martin et al., 2018; Lindsey et al., 2019; Zhu et al. 2020). Recent
 67 studies reported new recordings of vehicles, footsteps, and music, highlighting the sensitivity of
 68 DAS equipped dark fibers in the cities (e.g., Wang et al., 2020; Lindsey et al., 2020; Zhu et al.,
 69 2020).

70 Here we demonstrate the use of seismic recordings from an underground telecommunication
 71 fiber-optics DAS array in the cite of State College, PA, USA (Figure 1a) to reveal details of
 72 seismic noise variation caused by COVID-19 measures during March to June 2020. The timeline
 73 of the COVID-19 measures in State College, PA is summarized in Text S1. We show that
 74 seismic noises from 0.01 Hz to 100 Hz along the array are systematically impacted by the level
 75 of COVID-19 measures. We ascribe the noise reduction to the very-restrict stay-at-home and the
 76 noise recovery to less-restrict Phase Yellow/Green in State College. The linear correlation
 77 between seismic noises data and Google mobility data suggest that the use of seismic noise
 78 recordings by cite widely-installed infrastructure fiber optics provide a new way to quantify the
 79 level of human activities with high spatiotemporal resolution in a city.



80

81 **Figure 1.** (a): DAS map. Dark fiber (Green line) is located beneath Pennsylvania State
 82 University campus in State College, Pennsylvania (inset, red triangle). Selected channels are
 83 indicated for referencing sensors' location. Blue start indicates the construction site. (b):
 84 Temporal variation of seismic noise across the DAS channels with showing the timeline of local
 85 conditions above. Red line marks the abrupt noise change during the implementation of stay-at-
 86 home order. Clear diurnal pattern shows that signals are mainly from human activities at daytime.

87 2 Calculation of the RMS noise level

88 We examine seismic noise data (March 3 – June 10 2020) recorded by the DAS array connected
89 to underground telecommunication fiber optic cables, shown in Figure 1a. The DAS array makes
90 continuous strain rate measurements at a 500 Hz sampling frequency with a 10 m gauge length
91 and 2 m channel spacing, leading to all 2137 sensors along the array (detailed data description in
92 Text S2).

93 To quantify seismic noise in different frequency bands, we first calculate the noise power
94 spectral density (PSD) in each 5-minute window using McNamara’s method (McNamara, 2004).
95 We compute spectrograms, $A(\mathbf{f})$, by discrete Fourier transform. The PSD estimate, $P(\mathbf{f})$ is the
96 square of the spectrogram with a normalization factor:

$$97 \quad P(\mathbf{f}) = \frac{2\Delta t}{N} |A(\mathbf{f})|^2, \quad (1)$$

98 where Δt is the sampling interval (0.004 sec) and N is the number of data samples in each time
99 series segments. The PSD estimate for each hour is obtained by averaging 12 segment PSDs. In
100 this way, for each hour, we have a PSD estimate at each channel.

101 Then we calculate the RMS (root-mean-square) strain rate e_{rms} to represent the noise power by
102 taking the square-root of the integral of the power spectrum over four interested frequency bands,
103 0.1-1Hz, 1-10 Hz, 10-50 Hz and 50-100 Hz:

$$104 \quad e_{rms} = \sqrt{\int_{f_{min}}^{f_{max}} P(\mathbf{f}) d\mathbf{f}}, \quad (2)$$

105 Then the time-lapse noise change is defined as follows:

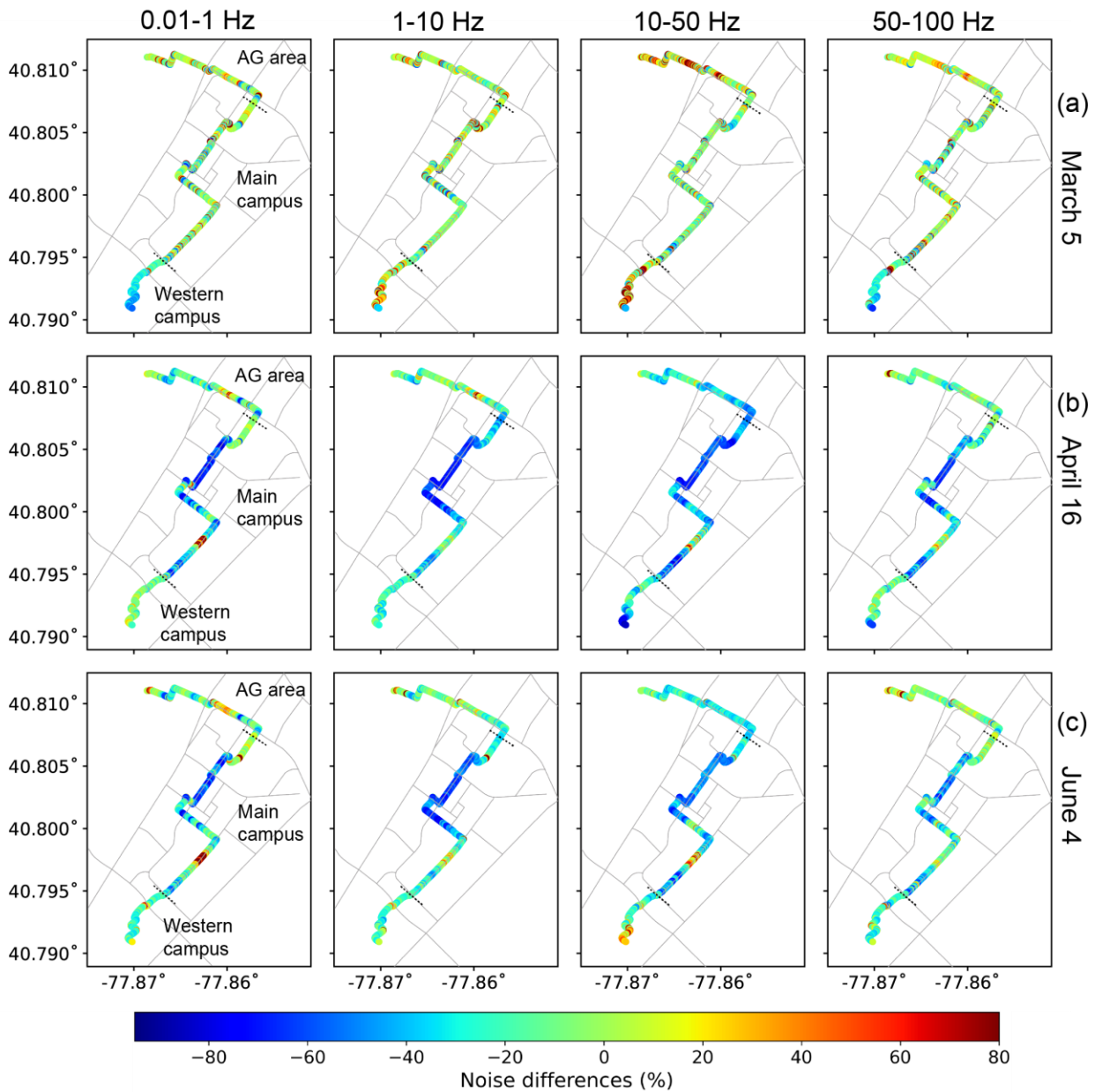
$$106 \quad N_{TL} = \frac{e_{rms} - e_{rms}^{baseline}}{e_{rms}^{baseline}} \times 100\%. \quad (3)$$

107 The baseline noise level $e_{rms}^{baseline}$ as reference is selected in the time period of 8 am to 6 pm and
108 is averaged over a week of spring semester (February 3-7 2020).

109 3 Spatial distribution of noise variation during COVID-19

110 We first present a meter-scale spatial variation of seismic noise (RMS strain rate) across the 5-
111 km DAS array, shown in Figure 1b. Spatially, during the entire period the seismic RMS noise
112 data was impacted mostly on the main campus, exhibiting the least variation in
113 agricultural/sports fields, and the intermediate variation on western campus. A significant drop of
114 seismic RMS noise is observed after the implementation of the stay-at-home measure (red line in
115 Figure 1b). After Phase Yellow seismic noise recovers but maintains at a relatively low level.

116 To understand the spatial variation of seismic noise in 2-meters spacing over the entire array, we
117 calculate the RMS strain rate over 10 hours from 8 am to 6 pm and then calculate the time-lapse
118 noise change on March 5 (spring semester), April 16 (during the stay-at-home measure) and June
119 4 (business reopening) (all Thursdays), to highlight seismic noise spatiotemporal variation
120 responding to different COVID-19 measures, shown in Figure 2. By analyzing noise in four
121 frequency bands (0.01-1 Hz, 1-10 Hz, 10-50 Hz, and 50-100 Hz), we aim to distinguish which
122 frequency band of noises is affected by the COVID-19 measures most.



123

124 **Figure 2.** Time-lapse noise variation across the DAS array. Time-lapse noise difference is
 125 calculated on a given day (top to bottom: March 5, April 16 and June 4 2020).

126

127 First, the biggest noise variation was detected on the main campus (Figure 2b). The peak noise
 128 reduction appears in all frequency bands on April 16 under the stay-at-home measure. This
 129 reduction is as much as 90% in the frequency band 1 – 10 Hz. With the gradual relaxation of the
 130 COVID-19 measure policies, the noise level on the main campus is increased but still stay at the
 131 lowest level (about 60% in 1-10 Hz).

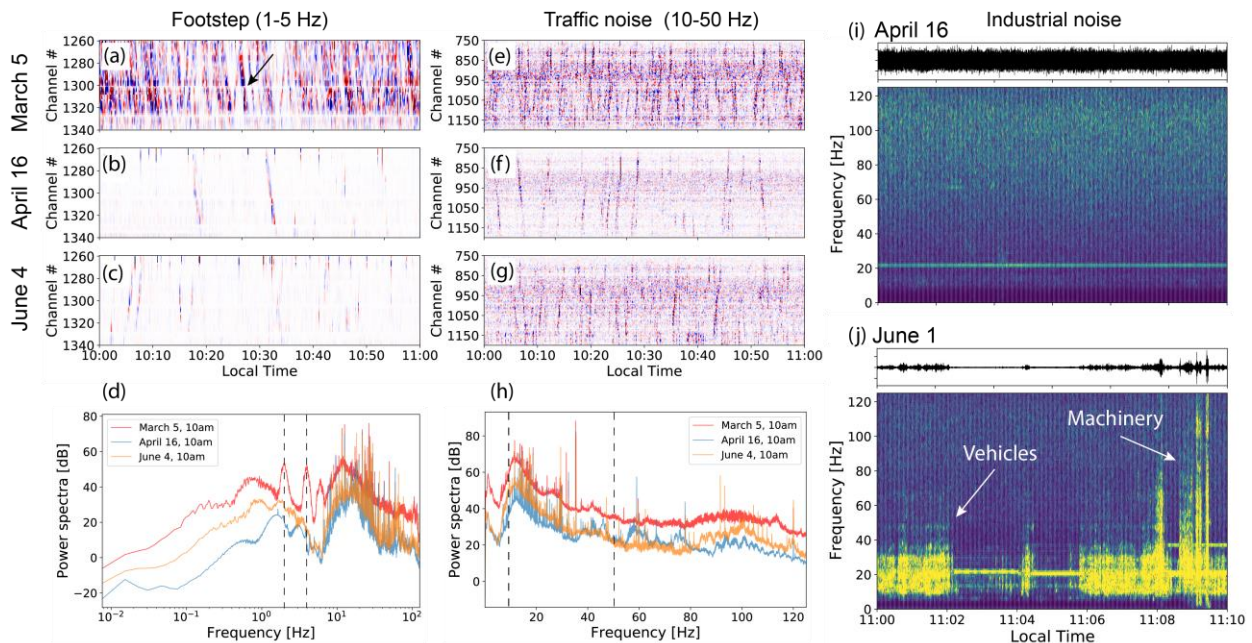
132 In the agricultural/sports fields and western campus with less school activities, the noise
 133 variation is relatively small in all frequency bands and the largest noise reduction is in 10 – 50
 134 Hz. This reduction could be caused by the decrease of traffics (e.g., school bus) due to the

135 COVID-19 measures. On the western campus, it is interesting to note that significant noise
 136 variation in the array end is likely caused by construction-associated human activities, i.e., shut-
 137 down of construction sites after the stay-at-home order and reopen of construction sites in Phase
 138 Green (details will be discussed in Figure 3).

139 We also find that channels just around the intersections detect large noise variation in the
 140 frequency band below 50 Hz while noise level of adjacent channels away from the road remains
 141 unchanged, which indicates that our fiber array is able to identify the exact places where traffic
 142 noise is dominant.

143 **4 Identification of noise sources associated with human activities**

144 Our dense DAS array at 2 m spacing enables us to identify noise sources – footstep signals,
 145 passing vehicles and industrial noise, by comparing seismic noise variation before and after the
 146 COVID-19 restriction. We select 1-hour data (local time 10 am – 11 am) from a subarray
 147 beneath a pedestrian-only path on the main campus at the same three days as section 3 (Figure 3).
 148 Intuitively, these linear events (arrow in Figure 3a) are walking signals appearing in almost every
 149 minute on March 5. After stay-at-home order was issued (April 16), very fewer linear signals
 150 (Figure 3b) can be seen on this path. In Phase Green (June 4), the footstep signals are almost not
 151 recovered despite of less restriction measures. This almost-no-recovery is confirmed by the
 152 average spectrum plot in Figure 5d, showing the absence of peaks at 2 Hz and 4 Hz in both April
 153 16 and June 4 curves, which are considered to be the footstep signals (Zhu et al., 2020).



155 **Figure 3.** DAS recordings and spectrums of footstep (a-d) and traffic noise (e-h) on March 5,
156 April 16, and June 4. Comparisons of construction-associated seismic noises in the stay-at-home
157 measure (April 16 2020) and in the Phase Green (June 1 2020). We select DAS recordings at
158 channel 2100 next to the construction site (its location is indicated in Figure 1a). Raw strain rate
159 data and their time-frequency spectra maps on (i) April 16 2020 and (j) June 1 2020.

160

161 Similar trend ‘decrease-increase’ can be found in traffic noise recordings (Figure 3e-h) from a
162 subarray beneath Curtin Road, the main road on campus. A significant decrease of passing
163 vehicles can be observed by comparing data on March 5 with April 16. This is because the
164 shutdown of the university prevented people from traveling to campus and the bus service was
165 also reduced. On June 4, a few more linear signals indicate more passing vehicles. This is
166 apparently different from almost-no-recovery of people movement. The frequency spectrum
167 (Figure 3h) confirms this trend: a significant drop of the power spectra between 10 - 50 Hz from
168 traffic vehicles about 30 dB, then an increase by 10 dB.

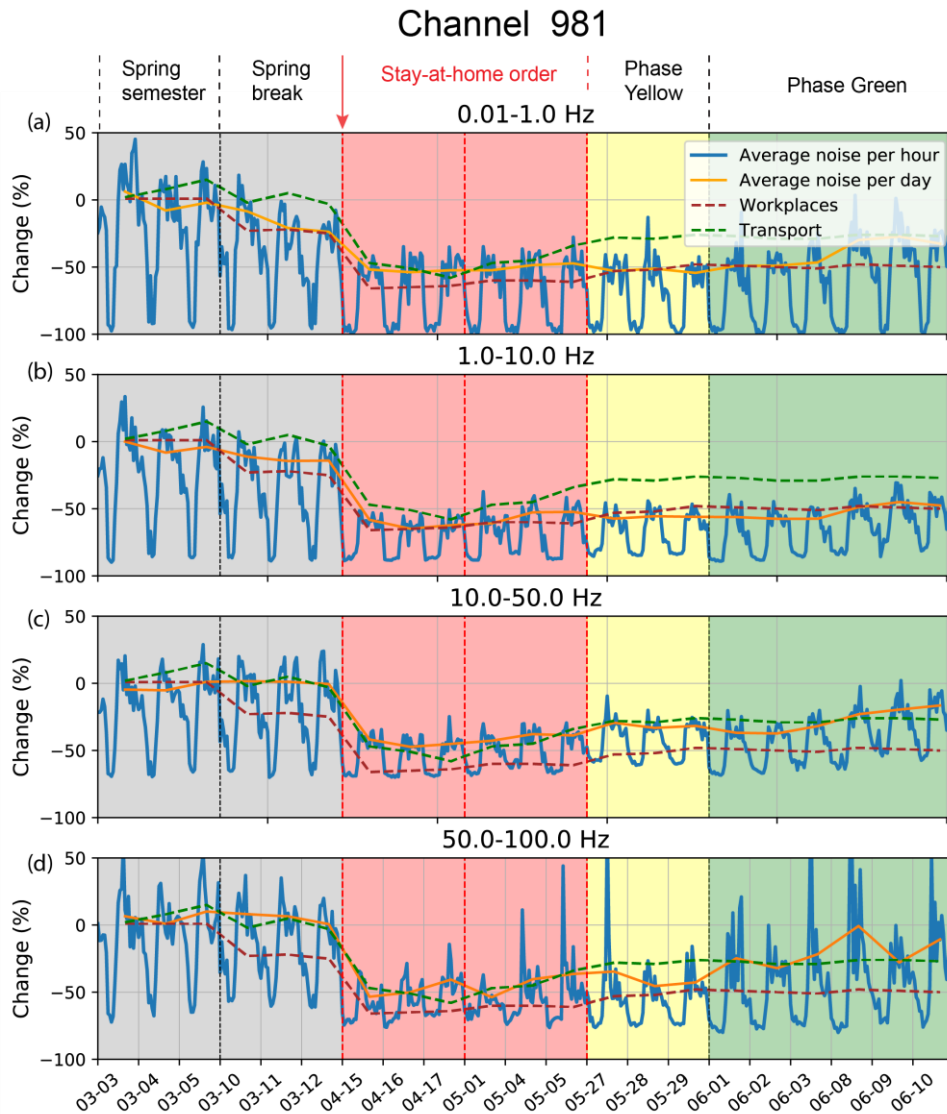
169 In addition, we find higher frequency noises associated with construction activities. On the
170 western campus, a new parking garage and utility upgrades nearby the fibers were planned to be
171 conducted from December 17, 2019 to April 20, 2021. Due to the suspension of the industrial
172 activity during the stay-at-home measures, the data on April 15 shows no detected events (Figure
173 3i). After re-opening industrial activities since May 7 (Phase Yellow), we can observe strong
174 industrial noises on June 1 in Figure 3j, which are identified in the spectra plot as the broadband
175 impulses (10 – 100 Hz) between 11:09 – 11:10 am from machines distinguished from the
176 construction vehicles noise in the frequency band of 10-30 Hz.

177

178 **5 Temporal noise variation during COVID-19**

179 While significant noise variation across the array is detected, we here show the complete
180 temporal noise variation from March 3 to June 10 2020.

181 Figure 4 shows the time-lapse noise change recorded by channel 981 located beneath Curtin
182 Road on the main campus (channel 204 in Figure S1 and channel 1491 in Figure S2). As a
183 comparison, all the results are plotted against the Google mobility data from workplaces and
184 transport (Text S3). First, we can see that noise experienced a slight drop (up to 10%) in the
185 spring break compared to normal spring semester in the low frequency band (0.01 - 10 Hz). In
186 10-50 Hz the noise change in both channel 981 (Figure 2c) and channel 1491 (Figure S2c)
187 remains flat before the stay-at-home order while the change in channel 204 (Figure S1) drops
188 down. In the high-frequency range (50-100 Hz) the noise change drops down only in channel
189 1491 (Figure S2d). We interpret that the reduction of low frequency noise (<10 Hz) is attributed
190 to least school activities during spring break (i.e., many students left school and there were few
191 school activities). The only reduction in the intermediate frequency (10-50 Hz) primarily caused
192 by traffics may be due to lack of school activities (e.g., reduced services of daily school buses)
193 and the stop of the machinery noise (probably from a construction site nearby channel 1491) may
194 cause the drop in Figure S2d.



195

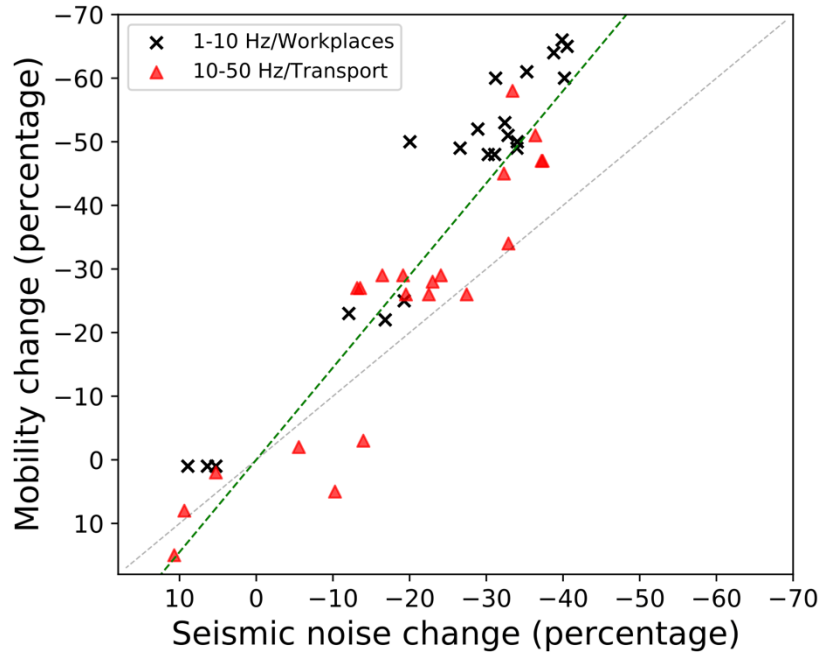
196 **Figure 4.** Noise change at channel 981 in the frequency range of (a) 0.01-1 Hz, (b) 1-10 Hz, (c)
 197 10-50 Hz and (d) 50-100 Hz. The daily average noise change (orange) as well as the mobility
 198 data provided by Google (dashed line) are plotted.

199

200 After the university closure on March 18, we observe a distinct drop (up to 60% daily average)
 201 of noise level falling to the lowest level in the whole period of the stay-at-home phase (Figures 2
 202 and S1 and S2). Moreover, this universal noise reduction in all frequency bands (0.01 – 100 Hz)
 203 reflects the quieter period and the disappearance of noise sources due to the stay-at-home order.
 204 There were almost no human activities.

205 After Phase Yellow on May 27, the noise level gradually recovered with less restriction
 206 measures. The noise level (0.01-10 Hz) still stay flat at the lowest level (50%~60% reduction)
 207 until the Phase Green. This feature implies that local residents still followed the stay-at-home
 208 order (e.g., working at home). Interestingly, the noise level (10-100 Hz) increase gradually,

209 which is similar to the mobility data (transport), suggesting the recovery of road traffics and
 210 industrial activities (e.g., shopping and construction business). After Phase Green, the noise in all
 211 frequency band gradually increases by a few percent (1-10 Hz) to 20% (0.01-1 Hz).



212
 213 **Figure 5.** Plot of time-lapse changes in seismic noise (1 - 10 Hz and 10 - 50 Hz) from all
 214 channels against with Google mobility data from workplaces and transport, respectively.

215
 216 To verify our seismic noise reduction, we adopt a similar strategy from previous studies (Lecoq
 217 et al., 2020) by using Google mobility data (Google, 2020), although the Google mobility data
 218 counts the whole Centre County and detailed information near the fiber is unavailable. Figure 5
 219 shows a crossplot between the noise data (daily average) and Google mobility data, including
 220 workplace and transit station (transport) in the Central County, PA (Text S3). The noise
 221 reduction in the frequency band of 1-10 Hz over all DAS channels is against the workplace
 222 mobility data while the 10-50 Hz noise level reduction is compared with transport mobility data.
 223 We can identify a linear correlation between mobility change and changes of seismic noise level
 224 with a ratio around 1.5. This linearity implies that the seismic noise variation (1-50 Hz) is
 225 linearly proportional to the amount of human activities including people movement and road
 226 traffics.

227 **6 Discussion and Conclusions**

228 Our study using dense fiber-optics seismic array offers high spatiotemporal details of seismic
 229 noise variation across the city of State College PA (USA) during the COVID-19 pandemic. Our
 230 results show a strong relation between seismic noise temporal variation and the timeline of the
 231 COVID-19 measures from stay-at-home (March-April 2020) to Phase Yellow/Green (May-June
 232 2020). Spatiotemporally, significant noise reduction as much as 90% in the frequency band 1-50
 233 Hz on the main campus is attributed to least local concentrated human activities (including

234 people movement and road traffic) due to the very-restrict stay-at-home measure in State College
235 PA. Similar noise reduction was also discovered in many other cities reported by previous
236 studies (Xiao et al., 2020; Poli et al., 2020; Lecocq et al., 2020; Dias et al., 2020; Yabe et al.,
237 2020).

238 In addition, our results reveal many new and detailed features of seismic noises caused by
239 progressive COVID-19 measures. First, the seismic noise variation in broad frequency bands
240 (0.01 – 100 Hz) shows the ‘decrease-increase’ trend, which is caused by ‘decrease-increase’
241 human activities during stay-at-home (March-April 2020) and Phase Yellow/Green (May-June
242 2020). This trend correlates well with the county mobility data released by Google (Google,
243 2020). Second, in Phase Yellow, the noise stay-flat (0.01-10 Hz) implies that local residents still
244 followed the stay-at-home order (e.g., less people movement) while the rapidly increased noise
245 level (10-100 Hz) implies the recovery of road traffics and industrial activities (e.g., shopping
246 and construction business). Third, seismic noises at frequencies below 1 Hz where anthropogenic
247 noise is weaker are also impacted by the COVID-19 measures which was not reported in
248 previous studies using seismometers (Xiao et al., 2020; Lecoq et al., 2020; Poli et al., 2020). We
249 note that, Lindsey et al. (2020) also observed a reduction in the very-low-frequency seismic
250 noise (0.01 – 1 Hz) using fiber sensors in Stanford, CA during COVID-19, and proposed that this
251 reduction is likely to be the geodetic response of the roadbed to decreased vehicle loading
252 (Jousset et al., 2018). This discovery may provide an additional constraint to quantify the number
253 of passing vehicles using dense seismic noise data. Furthermore, our results of the time-lapse
254 noise variation reveal the noise reduction zones in the kilometer scale. In the local noise
255 reduction zone (main campus) we can distinguish footsteps, single passing vehicle, and high-
256 frequency industrial noises associated with construction activities.

257 A linear correlation between mobility change and changes of seismic noise level implies that
258 seismic noise could be used for quantifying human activities in a city. Looking forward, the
259 fiber-optics array using existing telecommunication fiber networks makes it much more cost-
260 effective and practical in urban areas than other types of seismic sensors. This suggest the
261 superior of using city infrastructure fiber-optic cables to the mobility data for monitoring and
262 quantifying the human activity in a city (e.g., estimation of people movement and the number of
263 vehicles) with high spatiotemporal resolution. The high-resolution quantification could further
264 serve as an innovative approach for evaluating the impact of the COVID-19 measures in
265 populated areas.

266 In summary, our results show key connections between the progressive COVID-19 measures and
267 spatiotemporal seismic noise changes using a dense fiber array in a city scale. One implication of
268 this research is that seismic noise recorded by infrastructure DAS fiber networks could be a
269 factor considered by policy makers to monitor the effectiveness of measures and compliance of
270 the population with these mobility restrictions and optimize the COVID-19 measures in the
271 future pandemic.

272

273 **Acknowledgments**

274 We thank Chris Marone for his warm support to convince the Penn State Institute of Natural Gas
275 Research to provide seed money to the DAS fiber array. We thank Todd Myers, Ken Miller at
276 Penn State University, Thomas Coleman from Silixa Inc. who help setup the fiber-optic DAS

277 array. The DAS array was supported by Penn State Institute of Environment and Energy seed
278 grant and Institute of Natural Gas Research. Figure 1a is plotted with ArcGIS Pro.

279

280 **Data Availability Statement**

281 The DAS data used in this paper are available for download (at
282 <https://doi.org/10.5281/zenodo.4072484>)

283

284 **References**

285 Ajo-Franklin, J. B., Dou, S., Lindsey, N. J., Monga, I., Tracy, C., Robertson, M., et al. (2019).
286 Distributed Acoustic Sensing Using Dark Fiber for Near-Surface Characterization and
287 Broadband Seismic Event Detection. *Scientific Reports*, 9(1). [https://doi.org/10.1038/s41598-
288 018-36675-8](https://doi.org/10.1038/s41598-018-36675-8)

289 Bonnefoy-Claudet, S., Cotton, F., & Bard, P.-Y. (2006). The nature of noise wavefield and its
290 applications for site effects studies. *Earth-Science Reviews*, 79(3–4), 205–227.
291 <https://doi.org/10.1016/j.earscirev.2006.07.004>

292 Dias, F. L., Assumpção, M., Peixoto, P. S., Bianchi, M. B., Collaço, B., & Calhau, J. (2020).
293 Using Seismic Noise Levels to Monitor Social Isolation: An Example From Rio de Janeiro,
294 Brazil. *Geophysical Research Letters*, 47(16). <https://doi.org/10.1029/2020gl088748>

295 Google (2020). COVID-19 Community Mobility Reports. Available
296 at: <https://www.google.com/covid19/mobility/> (accessed: 25 September 2020).

297 Gupta, S., Nguyen, T., Rojas, F. L., Raman, S., Lee, B., Bento, A., et al. (2020). Tracking Public
298 and Private Responses to the COVID-19 Epidemic: Evidence from State and Local Government
299 Actions. *National Bureau of Economic Research*. <https://doi.org/10.3386/w27027>

300 Jarvis, C. I., Van Zandvoort, K., Gimma, A., Prem, K., Klepac, P., et al. (2020). Quantifying the
301 impact of physical distance measures on the transmission of COVID-19 in the UK. *BMC*
302 *Medicine*, 18(1). <https://doi.org/10.1186/s12916-020-01597-8>

303 Jousset, P., Reinsch, T., Ryberg, T., Blanck, H., Clarke, A., Aghayev, R., et al. (2018). Dynamic
304 strain determination using fibre-optic cables allows imaging of seismological and structural
305 features. *Nature Communications*, 9(1). <https://doi.org/10.1038/s41467-018-04860-y>

306 Lecocq, T., Hicks, S. P., Van Noten, K., van Wijk, K., Koelemeijer, P., De Plaen, R. S. M., et al.
307 (2020). Global quieting of high-frequency seismic noise due to COVID-19 pandemic lockdown
308 measures. *Science*, 369(6509), 1338–1343. <https://doi.org/10.1126/science.abd2438>

309 Lindsey, N. J., Martin, E. R., Dreger, D. S., Freifeld, B., Cole, S., James, S. R., et al. (2017).
310 Fiber-Optic Network Observations of Earthquake Wavefields. *Geophysical Research Letters*,
311 44(23), 11,792–11,799. <https://doi.org/10.1002/2017gl075722>

312 Lindsey, N., T. Craig Dawe, and Jonathan B. Ajo-Franklin. (2019). Illuminating seafloor faults
313 and ocean dynamics with dark fiber distributed acoustic sensing. *Science* 366.6469 1103–1107.

- 314 Lindsey, N. J., Yuan, S., Lellouch, A., Gualtieri, L., Lecocq, T., & Biondi, B. (2020). City-Scale
315 Dark Fiber DAS Measurements of Infrastructure Use During the COVID-19 Pandemic.
316 *Geophysical Research Letters*, 47(16). <https://doi.org/10.1029/2020gl089931>
- 317 Martin, E. R., Huot, F., Ma, Y., Cieplicki, R., Cole, S., Karrenbach, M., & Biondi, B. (2018). A
318 seismic shift in scalable acquisition demands new processing: Fiber-optic seismic signal retrieval
319 in urban areas with unsupervised learning for coherent noise removal, *IEEE Signal Processing*
320 *Magazine*, 35, 31–40.
- 321 McNamara, D. E. (2004). Ambient Noise Levels in the Continental United States. *Bulletin of the*
322 *Seismological Society of America*, 94(4), 1517–1527. <https://doi.org/10.1785/012003001>
- 323 Poli, P., Boaga, J., Molinari, I., Cascone, V., & Boschi, L. (2020). The 2020 coronavirus
324 lockdown and seismic monitoring of anthropic activities in Northern Italy. *Scientific Reports*,
325 10(1). <https://doi.org/10.1038/s41598-020-66368-0>
- 326 Xiao, H., Eilon, Z. C., Ji, C., & Tanimoto, T. (2020). COVID-19 Societal Response Captured by
327 Seismic Noise in China and Italy. *Seismological Research Letters*, 91(5), 2757–2768.
328 <https://doi.org/10.1785/0220200147>
- 329 Yabe, S., Imanishi, K., & Nishida, K. (2020, July 28). Two-Step Seismic Noise Reduction
330 Caused by COVID-19 Induced Reduction in Social Activity in Metropolitan Tokyo, Japan.
331 Research Square. <https://doi.org/10.21203/rs.3.rs-48413/v1>
- 332 Wang, X., Williams, E. F., Karrenbach, M., Herráez, M. G., Martins, H. F., & Zhan, Z.
333 (2020). Rose Parade Seismology: Signatures of Floats and Bands on Optical Fiber. *Seismological*
334 *Research Letters*, 91 (4): 2395–2398. <https://doi.org/10.1785/0220200091>
- 335 Zhan, Z. (2020). Distributed Acoustic Sensing Turns Fiber-Optic Cables into Sensitive Seismic
336 Antennas. *Seismological Research Letters*, 91(1), 1–15. <https://doi.org/10.1785/0220190112>
- 337 Zhu, T., Shen, J., & Martin, E. R. (2020, June 29). Sensing earth and environment dynamics by
338 telecommunication fiber-optic sensors: An urban experiment in Pennsylvania USA. submitted.
339 *Solid Earth*. <https://doi.org/10.5194/se-2020-103>
- 340